Int. Agrophysics, 1992, 6, 65-76

THE RHEOLOGICAL MODEL OF SILT CLAY LOAM

A. Oida[1], *K. Triratanasirichai*[2]

[1]Faculty of Agriculture, Kyoto University, Kyoto, 606 Japan
[2]Faculty of Engineering, Khon Kaen University, Khon Kaen 40002, Thailand

A b s t r a c t. A five-element rheological model was applied for analysing the stress relaxation behaviour of silt clay loam soil. A triaxial test was conducted in order to determine the mechanical properties (Young's modulus and viscosity coefficient) of the soil. Mathematical analysis of the model was developed and analysed by the Finite Element Method (FEM). From the comparison of stress relaxation curves between an experimental and computed by FEM, it was found that the experimental time-dependent stress relaxation curve was in good agreement with the predicted one from the rheological model.

INTRODUCTION

Because of complexity of soils, it was very diffcult to explain satisfyingly certain problems of the effect of time in vehicle-soil interaction. Several rheological models, composed of linear springs in combination with linear and non-linear dashpots and slider, have been proposed to simulate a soil behavior under the action of sustained stress.

Awadhwal and Singh [1] developed a rheological model for wet (puddled as well as unpuddled) soil and named as Yield-Maxwell (Y-M) model. Each of the Y-M units in the model contains a yield element (shear pin) in parallel with the dashpot of a Maxwell model. The experimental stress relaxation curves of soil samples were compared with those predicted from the model. The observed and the predicted force were found to be in good agreement. Murayama and Shibata [3] proposed a model consisting of a Voigt model in parallel with a slider, whereas Schiffman [8] model contained a Voigt model in series with a Maxwell model. Shu and Jiang [9] applied a three-element Hooke-Kelvin model and a four-element Burgers model to predict the thrust of driving wheel of two-wheel tractor, whilst Ji *et al.* [2] applied the same model to predict the sinkages of tracked and wheeled vehicles. Results were good in agreement between the experiment and calculated values. Oida [4-7] studied a linear time-dependent viscoelastic behaviour of soil which were analysed by the Finite Element Method (FEM). A rheological three-element model, which is easily handled and represents rationally the actual viscoelastic behaviour of soil, was suggested to obtain the rheological constants and a constitutive equation of soil. The time-dependent sinkage of a rigid wheel on the soil was also simulated by the FEM, regarding the rigid wheel and the soil as one mechanical system and setting the axial load of the wheel as the load boundary condition. The author stated that the calculated results by FEM and rheological technique have to be verified by the measurement.

Then, it can be stated that the soil, non-homogeneous material, can be represented by rheological models to simulate its

time-dependent force deformation as well as the flow response. The information derived from the rheological models should contribute not only to the development of procedures and design of equipment to alleviate the problems which is impeding mechanized cultivation on wet land, but also to the set up of total model to clarify the interaction between plant root and soil.

THEORY

In this study, a rheological model as shown in Fig. 1(a) has been proposed to predict the time-dependent stress relaxation behaviour of the puddled soil. The model consists of a spring E_1 parallel to a dashpot η and another spring E_1 in series with a yield element and these four elements are in series with a spring E. The both subscripted E are elastic constants and η is the viscosity

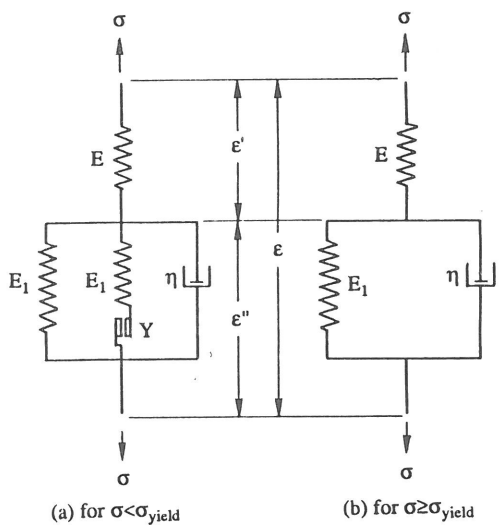

Fig. 1. Model of elasto-viscoplastic soil.

constant in the respective model. σ denotes an imposed stress at any time (t), and ε is a corresponding strain.

When a load is applied to the model and the stress is still less than yield stress, all spring and dashpot elements are in motion and we called it a 'Pre-Yield Response'. After the stress reaches the yield value, the yield element unlocks and the spring element E_1 (in series with the yield element) becomes an ineffective element, and we call it a 'Post-Yield Stress Relaxation'. Then the model will be reduced to a three-element model, as shown in Fig. 1(b).

For the model in Fig. 1(a), the stress-strain relations of the model for both strain parts (ε' and ε'') can be written in general form as follows:

$$\sigma = E\varepsilon' \text{ and } \sigma = 2E_1\varepsilon'' + \eta\dot{\varepsilon}''$$

Combining both equations and being converted into the normalized form of total strain, ε, the equation becomes as follows:

$$(E + 2E_1)\,\sigma + \eta\dot{\sigma} = 2E\,E_1\varepsilon + E\eta\dot{\varepsilon} \quad (1)$$

where the dot represents a differential with respect to time or it can be written as:

$$\left[1 + \left(\frac{\eta}{E + 2E_1}\right)\frac{d}{dt}\right]\sigma = \left[\frac{2E\,E_1}{E + 2E_1} + \left(\frac{E\,\eta}{E + 2E_1}\right)\frac{d}{dt}\right]\varepsilon \quad (2)$$

or rewritten in the form of arbitrary constant:

$$\left[1 + A\frac{d}{dt}\right]\sigma = \left[B + C\frac{d}{dt}\right]\varepsilon \quad (3)$$

where:

$A = \eta/(E + 2E_1)$

$B = 2EE_1/(E + 2E_1)$

$C = \eta\,E/(E + 2E_1)$.

Using the differential operators, Eq. (3) may be written as:

$$P\sigma = Q\varepsilon \quad (4)$$

where: P and Q are the differential operators and equal to $1 + A\frac{d}{dt}$ and $B + C\frac{d}{dt}$, respectively.

From the relation of stress tensor equation in the three-dimensional stress state, we can split the stresses into two parts as follows:

$$\begin{bmatrix} \sigma_x & \tau_{xy} & \tau_{xz} \\ \tau_{xy} & \sigma_y & \tau_{yz} \\ \tau_{xy} & \tau_{yz} & \sigma_z \end{bmatrix} = \begin{bmatrix} s & 0 & 0 \\ 0 & s & 0 \\ 0 & 0 & s \end{bmatrix} + \begin{bmatrix} s_x & s_{xy} & s_{xz} \\ s_{xy} & s_y & s_{yz} \\ s_{xz} & s_{yz} & s_z \end{bmatrix}$$

The first stress system on the right-hand side consists of equal tensile or compressive stresses and no shear, and it is called *hydrostatic stress*. The second term is called *stress deviator*. Its components are the stress deviations.

Corresponding to the above stress, the strain tensor equation is written as a matrix and split it just as we did for stresses:

$$\begin{bmatrix} \varepsilon_x & \varepsilon_{xy} & \varepsilon_{xz} \\ \varepsilon_{xy} & \varepsilon_y & \varepsilon_{yz} \\ \varepsilon_{xz} & \varepsilon_{yz} & \varepsilon_z \end{bmatrix} = \begin{bmatrix} e & 0 & 0 \\ 0 & e & 0 \\ 0 & 0 & e \end{bmatrix} + \begin{bmatrix} e_x & e_{xy} & e_{xz} \\ e_{xy} & e_y & e_{yz} \\ e_{xz} & e_{yz} & e_z \end{bmatrix}$$

The strain tensor above has split into one part which represents a pure *dilatation* (without change of shape), and into another part which represents a *distortion* or *strain deviator*, that is, a change of shape at constant volume.

The hydrostatic stress and strain are as follows:

$$s = \frac{1}{3}(\sigma_x + \sigma_y + \sigma_z),$$

$$e = \frac{1}{3}(\varepsilon_x + \varepsilon_y + \varepsilon_z). \qquad (5)$$

For the triaxial-symmetrical stress state then:

$$s = \frac{1}{3}(\sigma_x + 2\sigma_y) = \frac{1}{3}(\sigma_x + 2\sigma_3), \qquad (6)$$

because $\sigma_y = \sigma_z$ = confined pressure = σ_3, and the deviatoric stresses and strains are:

$$s_x = \sigma_x - s = \sigma_x - \frac{1}{3}(\sigma_x + 2\sigma_3)$$

$$= \frac{2}{3}(\sigma_x - \sigma_3),$$

$$s_y = \sigma_y - s = \sigma_y - \frac{1}{3}(\sigma_x + 2\sigma_3)$$

$$= -\frac{1}{3}(\sigma_x - \sigma_3),$$

$$e_x = \varepsilon_x - e = \varepsilon_x - \frac{1}{3}(\varepsilon_x + 2\varepsilon_y)$$

$$= \frac{2}{3}(\varepsilon_x - \varepsilon_y),$$

$$e_y = \varepsilon_y - e = \varepsilon_y - \frac{1}{3}(\varepsilon_x + 2\varepsilon_y)$$

$$= -\frac{1}{3}(\varepsilon_x - \varepsilon_y). \qquad (7)$$

If the viscoelastic material is isotropic, a relation between spherical stress and strain and that between distorsional stress and strain are written independently as follows:

$$P'' s = Q'' e,$$

$$P' s_x = Q' e_x, \qquad (8)$$

where P'', Q'', P' and Q' are differential operators and are independent of each other.

Substituting Eq. (7) into Eq. (8), then:

$$P''\left[\frac{1}{3}(\sigma_x + 2\sigma_3)\right] = Q''\left[\frac{1}{3}(\varepsilon_x + 2\varepsilon_y)\right],$$

$$P'\left[\frac{2}{3}(\sigma_x - \sigma_3)\right] = Q'\left[\frac{2}{3}(\varepsilon_x - \varepsilon_y)\right], \qquad (9)$$

or they are written for each ε_x and ε_y separately as follows:

$$(P''Q' + 2P'Q'')\sigma_x +$$

$$2(P''Q' - P'Q'')\sigma_3 = 3Q'Q''\varepsilon_x,$$

$$(P''Q' - P'Q'')\sigma_x +$$

$$(2P''Q' + P'Q'')\sigma_3 = 3Q'Q''\varepsilon_y. \qquad (10)$$

Volume change is assumed to be elastic, so that from Eq. (8):

$$P'' = 1, \quad Q'' = 3K \tag{11}$$

where K is called the modulus of compressibility. And it is also assumed that the shape variation is viscoelastic. Therefore, from Eq. (4):

$$P' = P = 1 + A\frac{d}{dt},$$

$$Q' = Q = B + C\frac{d}{dt}. \tag{12}$$

Then Eq. (10) becomes:

$$(Q + 6KP)\sigma_x + 2(Q - 3KP)\sigma_3 = 9KQ\sigma_x,$$

$$(Q - 3KP)\sigma_x + (2Q + 3KP)\sigma_3 = 9KQ\varepsilon_y. \tag{13}$$

In order to obtain the equation of stress relaxation when the strain ε_x changes like a unit step, Eq. (13) should be subjected to the Laplace transformations. That is:

$$(\overline{Q} + 6K\overline{P})\overline{\sigma}_x + 2(\overline{Q} - 3K\overline{P})\overline{\sigma}_3 = 9K\overline{Q}\,\overline{\varepsilon}_x. \tag{14}$$

Substituting $\overline{P} = 1 + As$, $\overline{Q} = B + Cs$, $\overline{\varepsilon}_x = \varepsilon_x/s$ and $\overline{\sigma}_3 = \sigma_3/s$ into Eq. (14), then:

$$[(B + Cs) + 6K(1 + As)]\overline{\sigma}_x + 2[(B + Cs) - 3K(1 + As)]\frac{\sigma_3}{s} = 9K(B + Cs)\frac{\varepsilon_x}{s}, \tag{15}$$

or

$$\overline{\sigma}_x = \frac{9K(B + Cs)\varepsilon_x}{s[(6KA + C)s + (6K + B)]} - \frac{2[(C - 3KA)s + (B - 3K)]\sigma_3}{s[(6KA + C)s + (6K + B)]}. \tag{16}$$

Taking a partial faction and an inverse Laplace transformation technique, the stress relaxation equation will be obtained as follows:

$$\sigma_x = \left[\frac{3EE_1}{\{E + (3 - 2\nu)E_1\}} + \frac{3E^2 e^{-2\frac{[E + (3 - 2\nu)E_1]}{\mu(3 - 2\nu)}t}}{(3 - 2\nu)\{E + (3 - 2\nu)E_1\}}\right]\varepsilon_x + \left[\frac{E + 4\nu E_1}{\{E + (3 - 2\nu)E_1\}} - \frac{3E(1 - 2\nu)e^{-2\frac{[E + (3 - 2\nu)E_1]}{\eta(3 - 2\nu)}t}}{(3 - 2\nu)\{E + (3 - 2\nu)E_1\}}\right]\varepsilon_3, \tag{17}$$

where: ν - Poisson's ratio, t - elasped time (s).

In order to obtain the rheological constants (E, E_1 and μ) the triaxial compression test of soil block was done as explained in the following section, and the time dependent stress relaxation curve was drawn as Fig. 2.

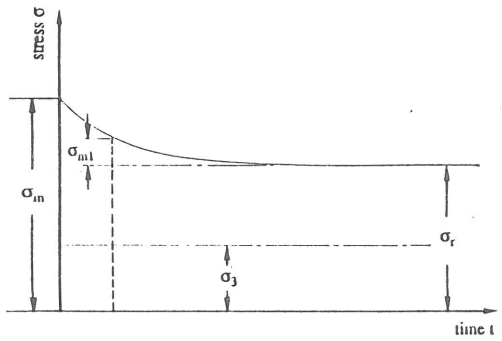

Fig. 2. The time-stress relaxation curve.

Selecting three elasped times, the stress values on the stress relaxation curve were obtained as follows:

$$\sigma_m \equiv \sigma_{x(t=0)} = \frac{3E}{(3 - 2\nu)}\varepsilon_x + \frac{4\nu}{3 - 2\nu}\sigma_3, \tag{18}$$

$$\sigma_r \equiv \sigma_x\ (t = \infty)$$

$$= \frac{3EE_1}{E + (3 - 2\nu)E_1}\varepsilon_x + \frac{E + 4\nu E_1}{E + (3 - 2\nu)E_1}\sigma_3 , \quad (19)$$

$$\sigma_{m1} \equiv \sigma_{x(t=t1)} - \sigma_{x(t=\infty)}$$

$$= \left[\frac{3E^2 e^{-2\frac{[E+(3-2\nu)E_1]}{\eta(3-2\nu)}t_1}}{(3 - 2\nu)\{E + (3 - 2\nu)E_1\}}\right]\varepsilon_x - \left[\frac{3E(1 - 2\nu)e^{-2\frac{[E+(3-2\nu)E_1]}{\eta(3-2\nu)}t_1}}{(3 - 2\nu)\{E + (3 - 2\nu)E_1\}}\right]\varepsilon_3 . \quad (20)$$

Then the rheological constants can be obtained from the equations above.

$$E = \frac{1}{3\varepsilon_x}[(3 - 2\nu)\sigma_m - 4\nu\sigma_3] ,$$

$$E_1 = \frac{[(3 - 2\nu)\sigma_m - 4\nu\sigma_3](\sigma_r - \sigma_3)}{3\varepsilon_x(3 - 2\nu)(\sigma_m - \sigma_r)} ,$$

$$\eta = \frac{2t[(3 - 2\nu)\sigma_m - 4\nu\sigma_3](\sigma_m - \sigma_3)}{3\varepsilon_x(3 - 2\nu)(\sigma_m - \sigma_r)\ln\left[\frac{\sigma_m - \sigma_r}{\sigma_{m1}}\right]} . \quad (21)$$

METHODS

Test apparatus

The triaxial compression test was conducted to determine the values of rheological parameters which define the strength and stress-strain-time characteristics of the soil subjected to a shear strain combined with compression. This device, shown in Fig. 3, consists of a confining chamber and a loading ram unit. The miniature load cells were used at the top and bottom platens inside the chamber. The axial displacement was measured with a linear variable differential transformer (LVDT) attached to the loading ram. The cell pressure was

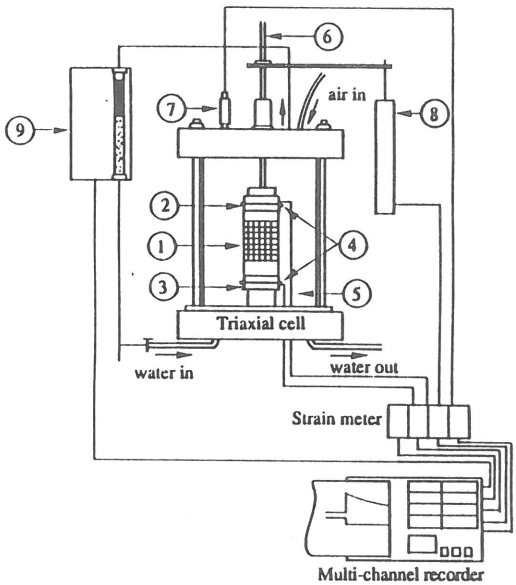

Fig. 3. Triaxial test apparatus. 1-soil specimen, 2-upper load cell, 3-lower load cell, 4-O-ring seals, 5-cell fluid, 6-loading ram unit, 7-pressure gauge, 8-linear variable differential transformer, 9-volume meter.

monitored by a fluid pressure transducer. During the test, the volume change of the test sample was measured by the water displacement and a photo-array system connected to the test chamber. The radial confinement of the sample was done with water under air pressure. The pressure supply unit consists of an air compressor connected with pressure measuring gages, precision pressure regulators and control valves.

Experiment procedure

A silt-clay-loam soil was prepared in the laboratory by an air drying, pulverized and passed through a 2 mm sieve. The sample was re-processed to obtain the required moisture contents by spraying atomized water with mixing and stirring by hand, and then sieved for an uniform distribution. The material was kept in air-tight plastic bags to get the equilibrium condition of desired moisture contents for several

days. About 200-350 g portion of the material was then poured into a 50 mm diameter cylindrical mold. According to the standard test of the soil, the sample was compacted in three layers of approximately equal thickness. The number of blows to compact the soil was varied with the required density. The sample was extruded into a split mold and the ends were trimmed with a wire trimmer to the required size of about 50 mm diameter, 100 mm long cylindrical sample.

The soil specimen with a thin rubber membrane with grid line was fixed to and it was confined by the pressure, σ_3 in the cell fluid. An axial load was applied to the samples by means of a loading ram, which had a good sliding fit with the hole drilled through the top of the cell, so that the pressure could be maintained in the cell during axial loading without significant leakage of cell fluid. By using a stepping motor with driver and controller unit, the axial force could be applied to the loading ram either at the controlled stress test or at the controlled strain test.

RESULTS

The experiment was conducted to determine the characteristic property of the soil sample under a constant deformation, i.e., under a stress relaxation test. The compressive force was applied to the sample at a certain deformation (2-4 mm). The deformation was kept constant for about 60-90 seconds. The force signals at the top and bottom of the specimen, deformation, confined pressure, volumetric change and the time-dependent strain change were simultaneously plotted out by a multi-channel data recorder as shown in Fig. 3. The output of stress relaxation was recorded until it attained to almost constant.

Fig. 4 shows an example of the result of stress relaxation test of the soil specimen with 44.02 % moisture content at various soil densities. After the load was applied to the specimen and the deformation was maintained at a constant level, the axial stress decreased rapidly until the elapsed time reached to 5 seconds. After that the stress still apparently decreased in accordance with the time. The sample was unloaded when the stress relaxation became constant or slightly decreased. The variation of density also affected to the result of the stress relaxation. The higher density caused the higher value of axial stress to maintain the constant deformation.

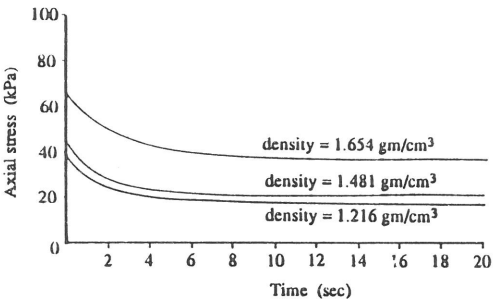

Fig. 4. The stress relaxation curves of the soil sample with different soil densities and 44.02 % moisture contents.

In the case that the soil moisture was varied (Fig. 5), test results showed interesting aspects. When the moisture content of the sample increased, the soil is likely a saturated material and difficult to shrink or to become more dense after the load was applied. This is because all pores are filled with water and the soil cannot be compacted any more. Then the soil particles will flow to the other ways, causing the lower stress is needed to maintain the deformation. The phenomena of the stress relaxation were also similar to the results which occurred in the lower moisture content tests.

Measured rheological parameters

The rheological constants of the model, E, E_1 and η have been evaluated from Eq. (21), utilizing the data of σ_m, σ_r, σ_3, σ_{m1}, ν and ε_x from the triaxial test which was described in the previous section.

The Young's modulus, E was plotted against the soil sample density for each soil

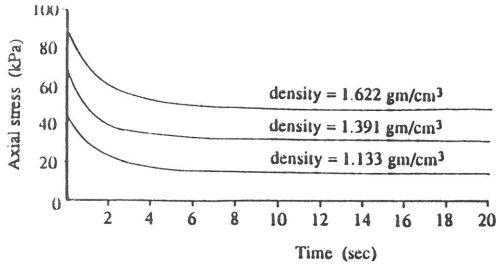

Fig. 5. The stress relaxation curves of the soil sample with different soil densities and 57.25 % moisture contents.

moisture content. A statistical analysis of the data revealed an apparent linear relation (r=0.91) between the value of E and the density. Examples of the results were plotted in Fig. 6 together with regression lines. It was observed that, for the results from the samples at 44.02 % moisture content, there was a sharper increase in the Young's modulus E than the sample at 57.25 % when the density increased. For example, there was an increase in E of 0.3 MPa for the sample with 44.02 % while the sample with 57.25 % gave that of 0.12 MPa for each 0.1 g cm^{-3} increase in density.

In the case of the Young's modulus E_1, it was found to be correlated with soil specimen density, as shown in Fig. 7. There was an overall increase in Young's modulus, E_1 of 0.2 MPa for each 0.1 g cm^{-3} increase in density of the sample at 44.02 % moisture content. While the result from the sample at 57.25 % showed 0.08 MPa increase in E_1 for each 0.1 g cm^{-3} increase in density.

Data in Fig. 8 indicated that the viscosity coefficient η linearly increased with an increase in density of soil specimen. The effect of the chosen elasped time for calculation was also shown in the same figure. As the chosen elasped time increased, the viscosity coefficient decreased gradually. These results were shown for both 44.02 % and 57.25 % moisture contents.

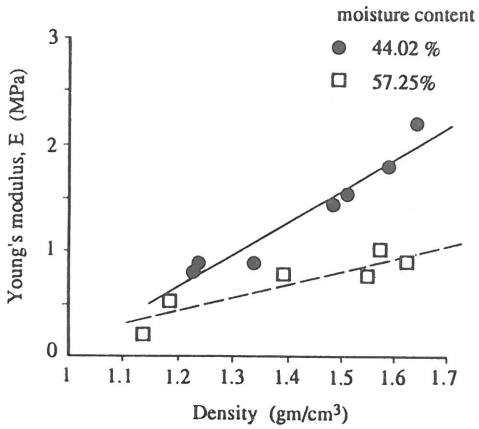

Fig. 6. Relationship between Young's modulus E and density.

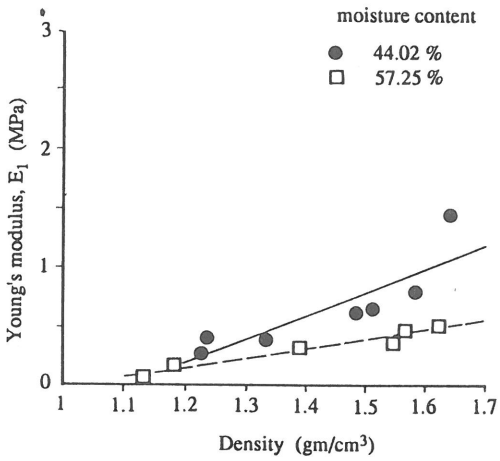

Fig. 7. Relationship between Young's modulus E_1 and density.

Mathematical analysis

As the author presented, the model was divided into 2 parts. Then, in order to apply this model to the prediction of stress relaxation behaviour, the mathematical analysis of each part should be done individually as follows.

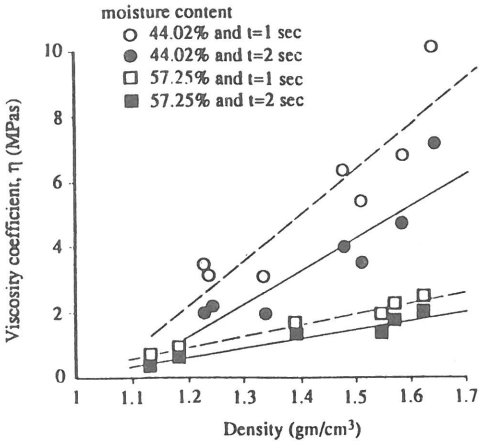

Fig. 8. Relationship between viscosity coefficient η and density.

For the case of Pre-Yield Response ($\sigma < \sigma_{yi}$)

Applying the Laplace transform to Eq. (8), then

$$\begin{aligned} \overline{P}'' s &= \overline{Q}'' e , \\ \overline{P}' s_x &= \overline{Q}' e_x . \end{aligned} \tag{22}$$

On the other hand, for the complete elastic body, which is a special case of rheological body:

$$\begin{aligned} s &= K(\varepsilon_x + \varepsilon_y + \varepsilon_z) = 3Ke , \\ s_x &= G\gamma = 2Ge_x , \end{aligned} \tag{23}$$

where K - coefficient of volumetric elasticity, G - shear modulus.

Comparing Eq. (23) with Eq. (22), the following correspondence can be done:

$$\begin{aligned} 3K &\Leftrightarrow \frac{\overline{Q}''}{\overline{P}''} , \\ 2G &\Leftrightarrow \frac{\overline{Q}'}{\overline{P}'} . \end{aligned} \tag{24}$$

By the above replacement the equation for the complete elastic body becomes perfectly the same as the Laplace transformed equation for the rheological body. Equation (24) is called the correspondence principle between the elastic and rheological problems. In other words the plane problem for the elastic body can be changed to the plane problem for the rheological body, using the correspondence principle. First, equations of Young's modulus, E and Poisson's ratio, ν correspond to the following equations of Laplace transformed differential operators:

$$\begin{aligned} E &= \frac{9KG}{3K+G} \Leftrightarrow \frac{3\overline{Q}'\overline{Q}''}{2\overline{P}'\overline{Q}'' + \overline{Q}'\overline{P}''} , \\ \nu &= \frac{3K-2G}{2(3K+G)} \Leftrightarrow \frac{\overline{P}'\overline{Q}'' - \overline{Q}'\overline{P}''}{2\overline{P}'\overline{Q}'' + \overline{Q}'\overline{P}''} . \end{aligned} \tag{25}$$

The relationship of the two-dimensional stress-strain for a complete elastic material can be presented by the following equations:

$$\begin{aligned} \sigma_x &= \frac{E}{1-\nu^2}(\varepsilon + \nu\varepsilon_y) , \\ \sigma_y &= \frac{E}{1-\nu^2}(\nu\varepsilon_x + \varepsilon_y) , \\ \tau_{xy} &= G\gamma_{xy} . \end{aligned} \tag{26}$$

Instead of E and ν, using the corresponding Laplace transformed differential operators, the rheological stress-strain relationships are written as follows in Laplace transforms:

$$\begin{aligned} &\overline{P}'(\overline{P}'\overline{Q}'' + 2\overline{Q}'\overline{P}'')\overline{\sigma}_x = \\ &\overline{Q}'[(2\overline{P}'\overline{Q}'' + \overline{Q}'\overline{P}'')\overline{\varepsilon}_x + (\overline{P}'\overline{Q}'' - \overline{Q}'\overline{P}'')\overline{\varepsilon}_y] , \\ &\overline{P}'(\overline{P}'\overline{Q}'' + 2\overline{Q}'\overline{P}'')\overline{\sigma}_x = \end{aligned}$$

$$\overline{Q}'[(\overline{P}'\overline{Q}'' + \overline{Q}'\overline{P}'')\overline{\varepsilon}_x + (2\overline{P}'\overline{Q}'' - \overline{Q}'\overline{P}'')\overline{\varepsilon}_y],$$

$$\overline{P}'\,\overline{\tau}_{xy} = \frac{\overline{Q}'\,\overline{\gamma}_{xy}}{2}. \tag{27}$$

Substituting
$\overline{P}' = 1 + As$, $\overline{Q}' = B + Cs$, $P'' = 1$ and $\overline{Q}'' = 3K$ into Eq. (27), and assuming that the deformation of the model is varied like a unit step function, then $\overline{\varepsilon}_x = \varepsilon_x/s$ and $\overline{\varepsilon}_y = \varepsilon_y/s$. Then:

$$[(3KA + 2C)s + (3K + 2B)]\overline{\sigma}_x =$$

$$\frac{(B + Cs)}{(1 + As)}\left[\{(6KA + C)s + (6K + B)\}\frac{\varepsilon_x}{s}\right] +$$

$$\left[\{(3KA - C)s + (3K - B)\}\frac{\varepsilon_y}{s},\right]$$

$$[(3KA + 2C)s + (3K + 2B)]\overline{\sigma}_y =$$

$$\frac{(B + Cs)}{(1 + As)}\left[\{(3KA - C)s + (3K - B)\}\frac{\varepsilon_x}{s}\right] +$$

$$\left[\{(6KA + C)s + (6K + B)\}\frac{\varepsilon_y}{s},\right]$$

$$\overline{\tau}_{xy} = \frac{(B + Cs)}{2(1 + As)}\frac{\overline{\gamma}_{xy}}{s}. \tag{28}$$

By the inverse Laplace transformation technique and substituting $K = \frac{1}{3}\frac{E}{1 - 2\nu}$ into the equations above, Eq. (28) becomes as follows:

$$\sigma_x = \left[\frac{4EE_1\{E + (3 - 2\nu)E_1\}}{(E + 2E_1)\{E + 2E_1(3 - 4\nu)\}} + \frac{E^2}{2(E + 2E_1)}e^{-\frac{E + 2E_1}{\eta}t} + \frac{3E^2 e^{-\frac{E+2E_1(3-4\nu)}{\eta(3-4\nu)}t}}{2(3 - 4\nu)\{E + 2E_1(3 - 4\nu)\}}\right]\varepsilon_x +$$

$$\left[\frac{2EE_1(E + 4E_1\nu)}{(E + 2E_1)\{E - 2E_1(3 - 4\nu)\}} - \frac{E^2}{2(E + 2E_1)}e^{-\frac{E + 2E_1}{\eta}t} + \frac{3E^2 e^{-\frac{E+2E_1(3-4\nu)}{\eta(3-4\nu)}t}}{2(3 - 4\nu)\{E + 2E_1(3 - 4\nu)\}}\right]\varepsilon_y, \tag{29}$$

or it is written in shorter form:

$$\sigma_x = a_{11}\varepsilon_x + a_{12}\varepsilon_y. \tag{30}$$

And also σ_y and τ_{xy} are written easily as follows:

$$\sigma_y = a_{12}\varepsilon_x + a_{11}\varepsilon_y,$$

$$\tau_{xy} = \left[\frac{EE_1}{E+2E_1} + \frac{E^2}{2(E+2E_1)}e^{-\frac{E+2E_1}{\eta}t}\right]\gamma_{xy} = a_{33}\gamma_{xy}. \tag{31}$$

Thus, the equation of stress relaxation of the 5-element model in the two-dimensional stress state in the case of visco-elastic deformation is as follows:

$$\begin{Bmatrix}\sigma_x\\ \sigma_y\\ \tau_{xy}\end{Bmatrix} = \begin{bmatrix}a_{11} & a_{12} & 0\\ a_{12} & a_{11} & 0\\ 0 & 0 & a_{33}\end{bmatrix}\begin{Bmatrix}\varepsilon_x\\ \varepsilon_y\\ \gamma_{xy}\end{Bmatrix}. \tag{32}$$

The equivalent stress of homogeneous material in two-dimensional stress state is expressed as follows:

$$\sigma^2 = \frac{3}{2}(\sigma_x^2 + \sigma_y^2 + 2\tau_{xy}^2). \tag{33}$$

For the case of Post-Yield Stress Relaxation ($\sigma \geq \sigma_{yi}$)

The relations of stress and strain of the model can be concluded in this case as follows:

$$[(E + E_1) + \eta\frac{d}{dt}]\sigma = [EE_1 + E\eta\frac{d}{dt}]\varepsilon, \tag{34}$$

or

$$(1 + A_1 \frac{d}{dt})\,\sigma = (B_1 + C_1 \frac{d}{dt})\,\varepsilon\,, \quad (35)$$

where:
$A_1 = \eta/(E + E_1)$,
$B_1 = EE_1/(E + E_1)$,
$C_1 = \eta E/(E + E_1)$.

Substituting the expressions of above constants into Eq. (27), we obtain the equations of σ_x, σ_y and τ_{xy} as follows:

$$\sigma_x = \left[\frac{EE_1\,\{2E + E_1(3 - 2\nu)\}}{(E + E_1)\,\{E + E_1(3 - 4\nu)\}} + \frac{E^2}{2(E + E_1)} e^{-\frac{E + E_1}{\eta_1}t} + \frac{3E^2}{2(3 - 4\nu)\,\{E + 2E_1(3 - 4\nu)\}} e^{-\frac{E + E_1(3-4\nu)}{\eta_1(3-4\nu)}}\right]\varepsilon_x +$$

$$\left[\frac{EE_1\,\{E + 2\nu E_1\}}{(E + E_1)\,\{E + E_1(3 - 4\nu)\}} - \frac{E^2}{2(E + E_1)} e^{-\frac{E + E_1}{\eta_1}t} + \frac{3E^2}{2(3 - 4\nu)\,\{E + E_1(3 - 4\nu)\}} e^{-\frac{E + E_1(3-4\nu)}{\eta_1(3-4\nu)}t}\right]\varepsilon_y$$

$$= b_{11}\varepsilon_x + b_{12}\varepsilon_y\,. \quad (36)$$

σ_y can be written easily as follows:

$$\sigma_y = b_{12}\varepsilon_x + b_{11}\varepsilon_y\,. \quad (37)$$

Shear stress τ_{xy} is obtained similarly:

$$\tau_{xy} = \left[\frac{EE_1}{2(E + E_1)} + \frac{E^2}{2(E + E_1)} e^{-\frac{E + E_1}{\eta_1}t}\right]\gamma_{xy}$$

$$= b_{33}\gamma_{xy}\,. \quad (38)$$

Therefore, the equation of stress relaxation of the three-element model in the two-dimensional stress state becomes as follows:

$$\begin{Bmatrix}\sigma_x\\ \sigma_y\\ \tau_{xy}\end{Bmatrix} = \begin{bmatrix}b_{11} & b_{12} & 0\\ b_{12} & b_{11} & 0\\ 0 & 0 & b_{33}\end{bmatrix} \begin{Bmatrix}\varepsilon_x\\ \varepsilon_y\\ \gamma_{xy}\end{Bmatrix}. \quad (39)$$

A Finite Element Method (FEM), is expected to be the most powerful tool to solve soil stress and deformation problems under complex boundary conditions. Usually basic equations should be formulated by the incremental method and the FEM is also based on it. The relation between nodal force increments Δf and nodal displacement increments Δu is linear as follows:

$$\Delta f = [K]\,\Delta u, \quad (40)$$

where $[K]$ is called as the stiffness matrix.

The components of this matrix change in accordance with the mechanical states of soil in the process of soil deformation. Equation (32) or Eq. (39) is used to build the stiffness matrix. The procedure for predicting the time-dependent stress relaxation is shown schematically in Fig. 9.

A FEM mesh, as shown in Fig. 10, which represented the half plane with a unit thickness of soil block, had 200 mm width and the height of 800 mm for this analytical region. This region was divided into 32 triangular elements with 27 nodes. A constant deformation was applied only in y-direction. The confined pressure of 0.4 kg f cm^{-2} or equivalent to the force of 313.9 N was applied along the length of the sample in x-direction. By the assumption of uniform distribution of this force along the right side of FEM mesh, then the forces acting on node numbers 6, 9, 12, 15, 18, 21, and 24 are 39.24 N each and at the node numbers 3 and 27 they are only 19.62 N each. As the displacement boundary conditions, only the bottom point of the centre line of soil block, node number 25, is fixed.

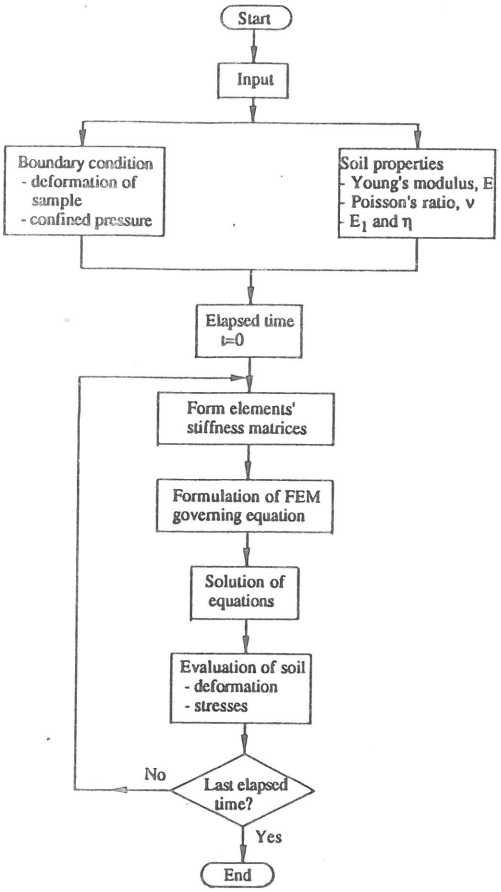

Fig. 9. The flow chart of Final Element Method program.

The other nodes on the centre line can move freely in y-direction but not in x-direction. The other nodes on the bottom line except node number 25 can only move in x-direction.

Comparison between calculated and measured stress relaxation curves

From the results of the computation above, the rheological constants are then utilized to predict the time-dependent stress relaxation curve of the sample by using the FEM program. The results from the calculation by FEM are shown in Fig. 11. Example of the results in this figure shows the comparison analysis between the computed stress by FEM and experimental curves of stress relaxation for soil specimen

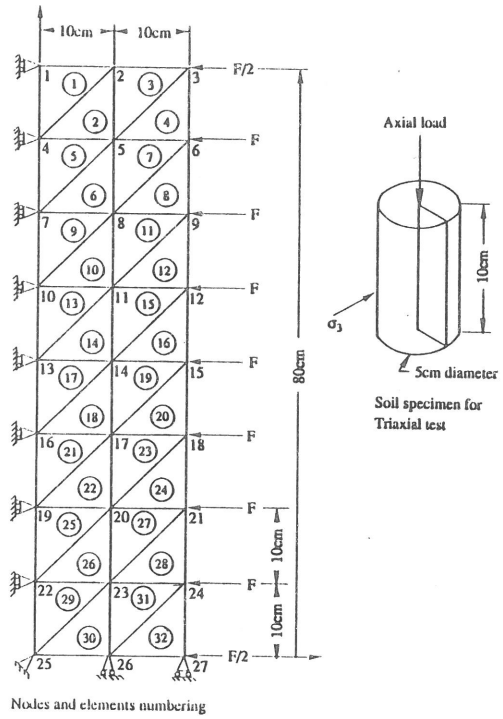

Fig. 10. Analytical model for Final Element Method.

with 1.622 g cm^{-3} of density and 52.25 % moisture content. From this figure it would be clear that the use of this rheological modelling and FEM program to predict the force or stress was successful from good agreement with the observed results.

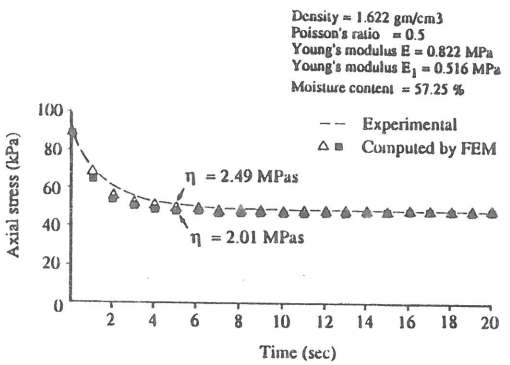

Fig. 11. The computed by FEM and experimental stress relaxation curves of the sample with 52.25 % moisture content.

There are, however, a little different values between the modelling and experimental curve. This would be caused by the assumption of constant viscosity coefficient. However, such a little error would be neglected in the practical work. For the other soil densities and moisture contents, the results also show a reasonably satisfactory prediction of the time-dependent stress relaxation behaviour of the triaxial test samples.

CONCLUSIONS

The rheological constants, Young's moduli, E, E_1 and viscosity coefficient (η) are linearly correlated to the specimen density. The results of rheological constants for high moisture content material showed lower value than in low moisture content. The viscosity coefficient was also affected by the elasped time, as an increase in elasped time caused a decrease in viscosity coefficient.

The load deformation and time-dependent stress relaxation behaviour of paddy soil can be represented by the proposed five-element rheological model. The experimental stress relaxation curves of soil samples were compared with those predicted by the FEM using the model and found to be in good agreement.

ACKNOWLEDGEMENT

This research was financially supported by the Ministry of Education, Science and Culture of Japan as Grant-in-Aid for Co-operative Research (Project No. 01304922).

REFERENCES

1. **Awadhwal N.K., Singh C.P.**: Mechanical and viscoelastic characteristics of paddled soil. Proc. Int. Conf. on Soil Dynamics, USA, Alabama, 3, 471-480, 1985.
2. **Ji C., Chen M., Pan J.**: Measurement of rheological parameters for paddy soils. Proc. 1st Asia-Pacific Conference of the ISTVS, Beijing, China, 445-456, 1986.
3. **Murayama S., Shibata T.**: On the rheological characteristics of clays. Part 1. Bulletin of Disaster Prevention Research Institute of Kyoto Univ., 26, 1958.
4. **Oida A., Yoshimura K.**: Analysis of viscoelastic behaviour of soil by means of Finite Element Method. Part 1. Determination of viscoelastic constants of soil (in Japanese). J. Japanese Soc. Agric. Machinery (JSAM), 41(3), 369-373, 1979.
5. **Oida A., Yoshimura K.**: Analysis of viscoelastic behaviour of soil by means of Finite Element Method. Part 2. Application of FEM in 2-dimensional stress state (in Japanese). J. Japanese Soc. Agric. Machinery (JSAM), 41(4), 553-558, 1979.
6. **Oida A., Tanaka T.**: Analysis of viscoelastic behaviour of soil by means of Finite Element Method. Part 3. Static sinkage of rigid wheel in Japanese. J. Japanese Soc. Agric. Machinery (JSAM), 43(1), 11-17, 1981.
7. **Oida A.**: Analysis of rheological deformation of soil by means of Finite Element Method. J. Terramechanics, 21(3), 237-251, 1984.
8. **Schiffman R.L.**: The use of viscoelastic stress-strain laws in soil testing. Am. Soc. Test. Material, Spec. Techn. Publ. (ASTM), No. 254, 1959.
9. **Shu Z., Jiang C.**: The research of rheological model of paddy field soil and its application. Proc. 1st Asia-Pacific Conference of the ISTVS, Beijing, China, 527-538, 1986.